NJC

Optical and magnetic properties of trans-indigo(.-) radical anions. Magnetic coupling between trans-indigo(.-) (S = 1/2) mediated by intermolecular hydrogen N-H...O=C bonds

Journal:	*New Journal of Chemistry*
Manuscript ID	NJ-LET-02-2019-000802.R1
Article Type:	Paper
Date Submitted by the Author:	28-Mar-2019
Complete List of Authors:	Konarev, Dmitri; Institute of Problems of Chemical Physics RAS, Zorina, Leokadiya; Institute of Solid State Physics RAS, Batov, Mikhail; Moscow State University, Khasanov, Salavat; Institute of Solid State Physics RAS, Otsuka, Akihiro; Research Center for Low Temperature and Materials Sciences, Kyoto University, Sakyo-ku, 606-8501, Yamochi, Hideki; Kyoto University, Kitagawa, Hiroshi; Kyoto University, Department of Chemistry Lyubovskaya, Rimma; Institute of Problems of Chemical Physics RAS,

SCHOLARONE™
Manuscripts

COMMUNICATION

Optical and magnetic properties of *trans*-indigo$^{\bullet-}$ radical anions. Magnetic coupling between *trans*-indigo$^{\bullet-}$ (S = 1/2) mediated by intermolecular hydrogen N-H···O=C bonds

Received 00th January 20xx,
Accepted 00th January 20xx

DOI: 10.1039/x0xx00000x

Dmitri V. Konarev,*[a] Leokadiya V. Zorina,[b] Mikhail S. Batov,[a, c] Salavat S. Khasanov,[b] Akihiro Otsuka,[d, e] Hideki Yamochi,[d, e] Hiroshi Kitagawa,[d] and Rimma N. Lyubovskaya[a]

Radical anion salt {cryptand[2.2.2](K$^+$)}$_6${*trans*-indigo}$_7$·5.5C$_6$H$_4$Cl$_2$ (1) with non-integer negative charge on indigo (–0.86 per molecule on average) was obtained. The salt manifests effective magnetic moment of 1.585 μ_B at 300 K and strong enough antiferromagnetic coupling of spins which can be mediated by intermolecular hydrogen bonds.

Introduction

Indigo is a well-known commercially produced dye.[1] Now indigo and its derivatives have found new application as electronic materials[2] and materials for rechargeable batteries[3]. Moreover, as a ligand for transition metals, indigo can coordinate to one and even two metal centers[4] and has different forms in these complexes. For example, indigo can change conformation from *trans*- to *cis*[4d, 4g-4h]. It can be deprotonated[4a-4c, 4e-4g]. This dye is redox active and potentially can form complexes in neutral, radical anionic and dianionic state[4d, 4h] (Scheme 1). Combination of deprotonation together with reduction[4e, 4f] or oxidation[4c, 4g] of indigo ligands is also possible. In these conditions it is important to know characteristics of an individual indigo molecule in different charged states to identify them in coordination complexes. Reduction of indigo is one of stages for the deposition of this dye on fabrics.[1] It is studied well electrochemically in solution.[5] However, till now reduced forms of indigo were not isolated in a crystalline form, and their molecular structure, optical and magnetic properties in solid state are still unknown.

In this work we studied the reduction of *trans*-indigo by potassium graphite in the presence of cryptand[2.2.2] and isolated crystalline radical anion salt {cryptand[2.2.2](K$^+$)}$_6${*trans*-indigo}$_7$·5.5C$_6$H$_4$Cl$_2$ (**1**) in which indigo preserves *trans*-conformation. Average negative charge on indigo is –0.86, and this charge is close to –1 indicating nearly radical anion state of this dye in **1**. In this work we studied the peculiarities of molecular structure, optical and magnetic properties of negatively charged *trans*-indigo which allow them to be identified in coordination complexes and other compounds.

Indigo in a neutral form adopts *trans*-conformation due to intramolecular hydrogen N-H···O=C bonds and the repulsion of carbonyl groups.[6] *Cis*-conformation of indigo is observed only in some coordination complexes.[4d, 4f-4h] As weak acceptor, indigo can be reduced to the radical anion state at the redox potential of -0.75 V *vs* Ag/AgCl (or -0.795 V *vs* SCE).[5] Therefore, strong donor like potassium graphite can easily produce radical anions of indigo. Since potassium graphite is completely insoluble in *o*-dichlorobenzene, we used cryptand[2.2.2] which forms stable complexes with alkali metal cations providing electron transfer from negatively charged graphite to indigo. We can carry out selective reduction using exactly one equivalent of cryptand[2.2.2] in each synthesis. Previously this method was used to prepare radical anion salts of different molecules like porphyrins, phthalocyanines, fullerenes, thioindigo and others.[7] In this study indigo was completely dissolved in *o*-dichlorobenzene during the reduction forming red-violet solution. Slow mixing with *n*-hexane produces crystalline salt {cryptand[2.2.2](K$^+$)}$_6${*trans*-indigo}$_7$ ·5.5C$_6$H$_4$Cl$_2$ (**1**). Composition of **1** was determined from X-ray diffraction on a single crystal. All the crystals were obtained as black blocks with characteristic copper luster. Several crystals tested from the synthesis show the same unit cell parameters, and therefore, it is concluded that only one crystal phase is formed. Elemental analysis confirms the composition of **1** (see SI).

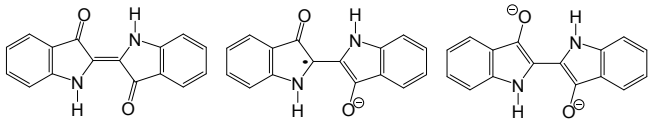

Scheme 1. Molecular structures of pristine *trans*-indigo as well its radical anion and dianion forms.

[a] Institute of Problems of Chemical Physics RAS, Chernogolovka, Moscow region, 142432 Russia, konarev3@yandex.ru;
[b] Institute of Solid State Physics RAS, Chernogolovka, Moscow region, 142432 Russia;
[c] Lomonosov Moscow State University, Leninskie Gory, Moscow, 119991 Russia;
[d] Division of Chemistry, Graduate School of Science, Kyoto University, Sakyo-ku, Kyoto 606-8502, Japan;
[e] Research Center for Low Temperature and Materials Sciences, Kyoto University, Sakyo-ku, Kyoto 606-8501, Japan.

Electronic Supplementary Information (ESI) available: experimental section, IR spectra of pristine compounds and salt **1**, EPR data. See DOI: 10.1039/x0xx00000x

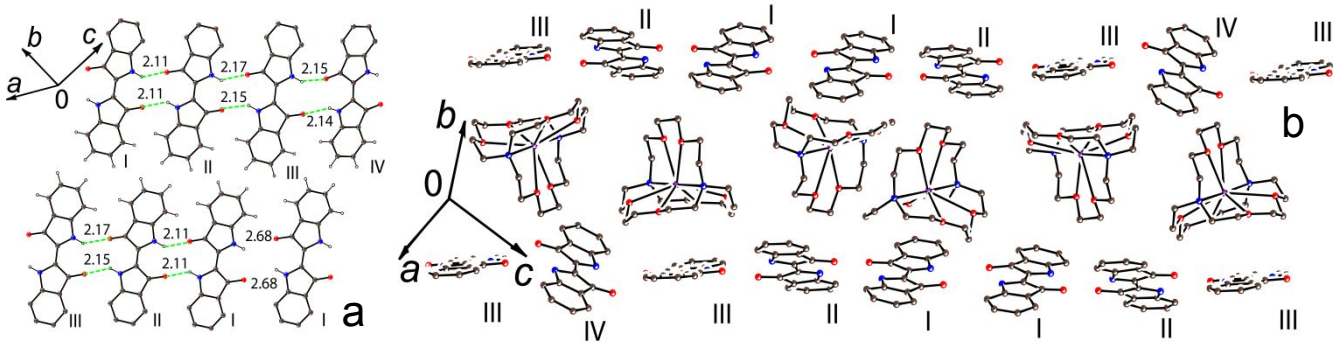

Fig. 1 Crystal structure of **1**: (a) view on the layer of the *trans*-indigo$^{\bullet-}$ radical anions. Short intermolecular N-H···O=C hydrogen bonds are shown by green dashed lines; (b) view along the indigo layers separated by bulky {cryptand[2.2.2](K$^+$)} cations (solvent molecules are not depicted).

Results and Discussion

Crystal structure of **1** studied at 120 K has a low-symmetry triclinic unit cell.[8] The composition of this salt is quite unusual since there are four independent indigo molecules – three with full occupancy and one with half occupancy positioned in the inversion center. At the same time there are three independent {cryptand[2.2.2](K$^+$)} cations and solvent $C_6H_4Cl_2$ molecules. Two of three solvent molecules have full occupancies and one molecule has the occupancy of 0.75. Therefore, the composition of **1** is {cryptand[2.2.2](K$^+$)}$_3${*trans*-indigo}$_{3.5}$·2.75$C_6H_4Cl_2$ or {cryptand[2.2.2](K$^+$)}$_6${*trans*-indigo}$_7$·5.5$C_6H_4Cl_2$. The complex has layered structure. The indigo$^{\bullet-}$ radical anions form closely packed layers among which weakly interacting chains can be outlined (Fig. 1a). These layers alternate with the cationic layers composed of the {cryptand[2.2.2](K$^+$)} cations (Fig. 1b). Small vacancies in the cationic layers are occupied by solvent $C_6H_4Cl_2$ molecules (not shown in Fig. 1b). Since {cryptand[2.2.2](K$^+$)} cations have large size and indigo molecules have smaller size, only limited number of cations can be accommodated in the cationic layers. We suppose that this is a reason for smaller content of cations and, hence, non-integer charge transfer to the indigo molecules in **1** (average charge is –0.86 per molecule). The chains formed by the indigo molecules can be outlined within the layers (Fig. 1a) in which strong intermolecular hydrogen bonds between the NH group and carbonyl oxygen atom are formed. There are groups from seven indigo molecules within the chains with short intermolecular (N)H···O(C) and N···O distances of 2.11-2.17 and 2.86-2.91 Å, respectively, indicating the formation of strong hydrogen bonds. At the same time the intermolecular (N)H···O(C) and N···O distances between indigo$^{\bullet-}$ from the neighboring groups are essentially longer (2.68 and 3.35 Å, respectively), indicating the absence of hydrogen bonds. Therefore, chains from indigo$^{\bullet-}$ are not continuous but contain large fragments bonded by strong hydrogen bonds. The absence of hydrogen bonds in one case can be explained by parallel arrangement of indigo$^{\bullet-}$ and their strong shift relative to each other. At the same time planes of radical anions forming strong hydrogen bonds are bent relative to each other (the dihedral angles between them are from 18 to 34^o). We suppose that the formation of hydrogen bonds is a main driving force for the aggregation of indigo in the chains and layers. It is interesting that related thioindigo dye cannot participate in the formation of hydrogen bonds. As a result the salt with 1:1 composition, namely, {cryptand[2.2.2](K$^+$)}(thioindigo)$^{\bullet-}$ has another packing motif in which thioindigo molecules form channels accommodating the {cryptand[2.2.2](K$^+$)} cations.[7d] In spite of a close approach of the indigo molecules in **1,** no effective π-π interaction was observed between them. There is only one side-by-side C···C contact (3.60 Å) between the phenylene groups of indigo$^{\bullet-}$ among the neighboring chains within a layer. Thus, salt **1** is an example of a structure in which radical anions are bonded mainly by strong intermolecular hydrogen bonds without essential π-π interaction between them.

Unit*	Central C=C bond, Å	Carbonyl C=O bond, Å	Single (C=)C-N bond, Å	Single (C=)C-C(=O) bond, Å	Twist angle,^{o}
Pristine *trans*-indigo[6b]	1.343(2)	1.239(2)	1.381(2)	1.460(2)	close to 0
Deprotonated (*cis*-indigo)$^{2-}$ dianion[4f]	1.370(2)	1.223(2)	1.385(2)	1.484(2)	7.9 (bend)
indigo$^{\bullet-}$ in **1** (labels are shown in Fig. 1) I	1.384(5)	1.240(5) 1.287(8)	1.361(5) 1.409(5)	1.466(6) 1.411(6)	6.6
II	1.381(5)	1.238(5) 1.281(5)	1.388(5) 1.411(4)	1.455(5) 1.407(5)	3.6
III	1.400(5)	1.254(4) 1.276(4)	1.377(4) 1.385(4)	1.450(4) 1.413(4)	4.7
half of IV	1.386(7)	1.267(4)	1.400(4)	1.444(5)	0

Table 1. Average bond lengths in pristine *trans*-indigo, salt **1** and reference compounds.

*the positions of the bonds are shown in Scheme 1 for neutral *trans*-indigo.

Indigo preserved *trans*-conformation at reduction in **1**. It is believed that reduction of indigo is accompanied by the elongation of C=O and central C=C bonds and shortening of the C(C=O)-C(C=C) bonds[5] which should be single and double bonds, respectively, in the dianionic state (Scheme 1). It is interesting to consider the distribution of negative electron density on indigo$^{\bullet-}$. It can be asymmetric when negative charge is positioned only on one half of the molecule but spin density of the radical anion is positioned mainly on another half of the molecule (as shown in Scheme 1). If there are two mixed resonance structures with negative charge in one or the other half of the molecule, the changes in bond lengths should be observed for both halves of the molecule. Bond lengths in pristine *trans*-indigo, reference compound and salt **1** are listed in Table 1. There are four independent indigo molecules labeled from I to IV in Fig. 1. It is seen that the central C=C bond is noticeably elongated at the reduction for molecules I-IV as predicted. At the

 This journal is © The Royal Society of Chemistry 20xx

same time rather asymmetric charge distribution is observed for molecules I and II since no changes in the bond length are observed for the C=O and C(C=O)-C(C=C) bonds in one half of the molecule (the length of these bonds is nearly the same as in neutral *trans*-indigo, Table 1). However, these bonds are noticeably elongated and shortened, respectively, for the other half of the molecule indicating that negative charge is localized mainly on this half. The changes in bond length are observed for both halves of the molecule for molecule III only but this effect is greater for one half than for the other half of the molecule (Table 1). The changes in bond length expected for the reduction are also found for the molecule of type IV. The occupancy of the molecule is 0.5. However, the bonds of both halves of the molecule are identical in symmetry (Table 1). Thus, structural analysis shows that negative electron density is distributed quite asymmetrically in the main part of the indigo units and is localized mainly in one half of the molecule. Pristine *trans*-indigo has nearly planar shape[6b] but the formation of indigo$^{\bullet-}$ in **1** is accompanied by a slight increase in twist angle between two halves of the molecule up to 3.6-6.6° (Table 1). Twist angle is equal to 0° for indigo molecule IV only due to symmetry requirement.

Deprotonation of indigo which is accompanied by the formation of mono- or dianions does not allow the formation of hydrogen bonds. Besides this, the effect of deprotonation on geometry of indigo is opposite to the reduction – the C=O bonds are shortened but the C(C=O)-C(C=C) bonds are even elongated in comparison with pristine *trans*-indigo[4f] (see Table 1). Obviously, there is no deprotonation in **1** since the main part of indigo molecules in this salt is involved in the formation of strong hydrogen bonds with the neighbors (Fig. 1a) and the changes in bond lengths for all independent indigo molecules in **1** indicate their reduction. These charges are opposite to those observed for the deprotonated indigo[4f].

IR spectra of pristine *trans*-indigo and salt **1** are shown in Fig. S1, and the positions of the bands are listed in Table S1. Spectrum of **1** is a superposition of the bands of indigo, cryptand[2.2.2](K$^+$) cations and solvent $C_6H_4Cl_2$ molecules. The bands of pristine *trans*-indigo at 1613 and 1627 cm^{-1} can be attributed to C=O stretching vibrations. The position of these bands remains unchanged in the spectrum of **1** and they are positioned at 1614 and 1625 cm^{-1} but their intensity decreases strongly. This is in a good agreement with asymmetric distribution of negative electron density in indigo$^{\bullet-}$ supposed by us since the geometry of one half of the molecule is very close to that in pristine *trans*-indigo (see crystal structure section). Essential elongation of the C=O bond in the other half of the molecule should result in a strong shift of this band to

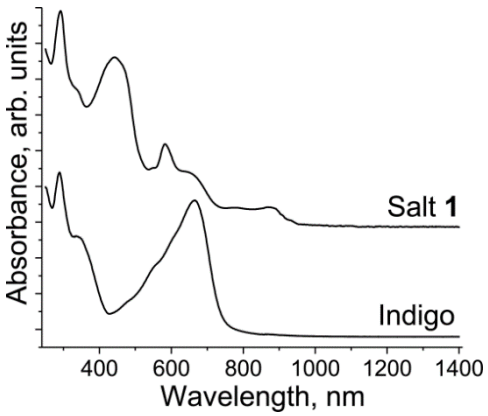

Fig. 2 Spectrum of pristine *trans*-indigo and salt **1** in the visible-NIR range in KBr pellets. Pellets for **1** were prepared in anaerobic conditions.

smaller wavenumbers. Therefore, a new intense band positioned in the spectrum of **1** at 1482 cm^{-1} can be attributed to vibrations of the carbonyl group.

Optical spectra of *trans*-indigo and salt **1** are shown in Fig. 2. *Trans*-indigo has intense absorption in the visible range with maximum at 665 nm (Fig. 2). This absorption is attributed to the S_0-S_1 transition.[9] There are also two weaker bands in the spectrum of *trans*-indigo at 287 and 331 nm (Fig. 2). The formation of **1** results in the appearance of new bands in the NIR range at about 790 and 880 nm. These bands appear due to population of LUMO orbital in indigo$^{\bullet-}$ (which becomes singly occupied molecular orbital (SOMO)) and the appearance of new transitions from this orbital to the vacant LUMO+1 orbital. Instead of an intense band in the visible range at 665 nm, salt **1** manifests essentially weaker bands at 581 and 637 nm and a broad intense band at 443 nm. Thus, absorption in the visible range for indigo$^{\bullet-}$ preserves positions of some bands (bands at 581 and 637 nm) but the main band is strongly blue shifted at reduction (this band is positioned at 443 nm). At the same time the band in the UV-range preserves position at 292 nm in the spectrum of **1** (Fig. 2).

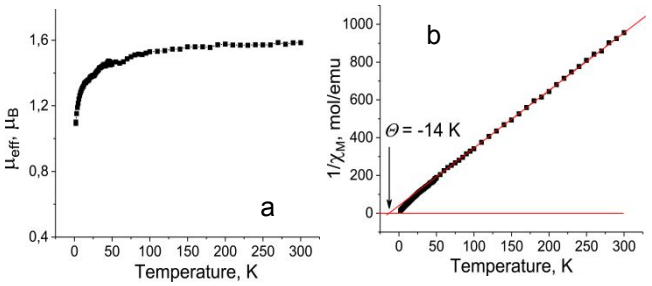

Fig. 3 Temperature dependences of (a) effective magnetic moment and (b) reciprocal molar magnetic susceptibility for polycrystalline **1**.

Magnetic properties of salt **1** were studied by both SQUID and EPR techniques. Effective magnetic moment is equal to 1.585 μ_B at 300 K per {cryptand[2.2.2](K$^+$)}$_{0.85}${*trans*-indigo}·0.79$C_6H_4Cl_2$ unit containing one indigo molecule (Fig. 3a). This value is smaller than the theoretical value of 1.73 μ_B calculated for the system with one noninteracting S = 1/2 spin per formula unit. The reason of that is a smaller degree of charge transfer to the indigo molecules in **1** (–0.86 on the average). If we take in account this fact, the

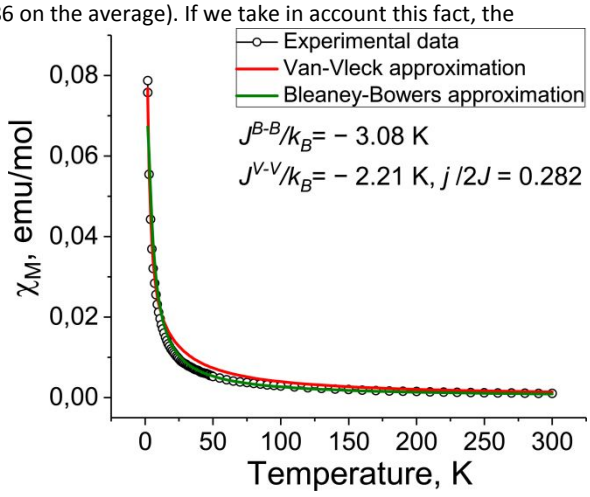

Fig. 4 Modeling of the magnetic behavior of **1** by using the Van-Vleck[10] and the Bleaney-Bowers[11] approximations.

calculated magnetic moment of 1.60 μ_B is rather close to the observed value. Reciprocal molar magnetic susceptibility is linear in the 50-300 K range allowing one to determine Weiss temperature by the Curie-Weiss fitting of the data as -14 K (Fig. 3b). This value indicates rather strong antiferromagnetic coupling of spins manifested in **1**.

Magnetic susceptibility of **1** was modeled using two different fits (Fig. 4), through which two magnetic coupling constants with closely matching values were obtained. The first approximation, the modified Van-Vleck expression[10] for a six-electron antiferromagnetic S = 1/2 spin system, has yielded a value of J/k_B = − 1.54 см$^{-1}$ = − 2.21 K , j = − 0.87 cm^{-1} with a rather large amplitude of $j/2J$=0.282, and g = 2.003. The second approximation − the Bleaney-Bowers equation[11] for a S = 1/2 system − provided a slightly better fit with the exchange constant J/k_B = − 2.14 cm^{-1} = − 3.08 K, g = 2.003. An attempt to treat the system as a finite 1D seven-membered alternating-exchange Heisenberg S = 1/2 spin chain and model it accordingly[12] failed to give any non-zero value of the *inter*-chain exchange constant, thus allowing one to assume that any interaction of such nature is being effectively suppressed.

Salt **1** contains blocks from seven indigo$^{\bullet-}$ bonded by strong intermolecular hydrogen bonds (Fig. 1a). We can suppose that magnetic coupling occurs namely in these blocks and, therefore, hydrogen bonds can rather effectively mediate magnetic coupling between S = 1/2 spins. That is also the reason for the decrease of effective magnetic moment of **1** at low temperatures (Fig. 3a).

Radical anions of *trans*-indigo$^{\bullet-}$ manifest a Lorentzian EPR signal with g = 2.0047 and a linewidth (ΔH) of 0.506 mT at 295 K (Fig. 5, inset). This signal is similar to that observed for the thioindigo$^{\bullet-}$ radical anions in {cryptand[2.2.2](K$^+$)}(thioindigo)$^{\bullet-}$ with g = 2.0051 and ΔH = 0.60 mT at 295 K. In case of thioindigo salt, the signal shows nearly temperature independent g-factor but linewidth of the signal is slightly broadened to 0.72 mT with the temperature decrease down to 4.2 K.[7d] The EPR signal of **1** exhibits the behavior similar to that for the (thioindigo)$^{\bullet-}$ salt. While the Lorentzian shape was preserved down to low temperatures, the slight shift of g-factor to smaller values (g = 2.0042 at 19 K, Fig. S2) and slight broadening (6.20 mT at 19 K, Fig. 5b) were observed. The temperature dependence of integral intensity of the EPR signal can be fitted well by the Curie-Weiss law with negative Weiss temperature of -12 K (Fig. 5a) which is almost identical to that estimated from SQUID data (-14 K) (Fig. 3b).

Conclusions

In conclusion, the salt containing indigo$^{\bullet-}$ radical anions was obtained for the first time in crystalline form as {cryptand[2.2.2](K$^+$)}$_6${*trans*-indigo}$_7$·5.5$C_6H_4Cl_2$ compound with non-integer charge transfer to the indigo molecules (–0.86 on the average). The salt has alternating layered structure consisting of the cationic layers and the indigo layers in which indigo$^{\bullet-}$ radical anions are bonded in the blocks from seven molecules by strong intermolecular hydrogen bonds. The reduction of *trans*-indigo elongates the carbonyl C=O bond and the central C=C bond, and shortens the C(C=O)-C(C=C) bonds. Negative electron density quite unsymmetrically distributed in a radical anion molecule is evidenced by the distinct bond length modulation in one half of the molecule, whereas the geometry of the other half of the molecule remains unchanged relative to pristine *trans*-indigo. The reduction gives the new NIR bands and the shift of the intense band of indigo from 665 to 443 nm. The effective magnetic moment of **1** corresponds to the estimated value derived from the concentration of indigo$^{\bullet-}$ radical anions with the S = 1/2 spin state. The unpaired spin affords a narrow EPR signal. The origin of rather strong antiferromagnetic coupling between S = 1/2 spins of indigo$^{\bullet-}$ is supposed as a result of strong hydrogen bonds formed between the indigo$^{\bullet-}$ radical anions. Thus, together with π-π interactions, hydrogen bonding is also regarded as a rather effective route for magnetic coupling of spins in organic systems.

Fig. 5 EPR data for polycrystalline salt **1**: (a) temperature dependence of integral intensity of the signal (black circles) and fitting the data by the Curie-Weiss law with Weiss temperature of -12 K (red curve); (b) temperature dependence of linewidth of Lorentzian EPR signal. Inset shows the EPR signal from polycrystalline **1** at 295 K.

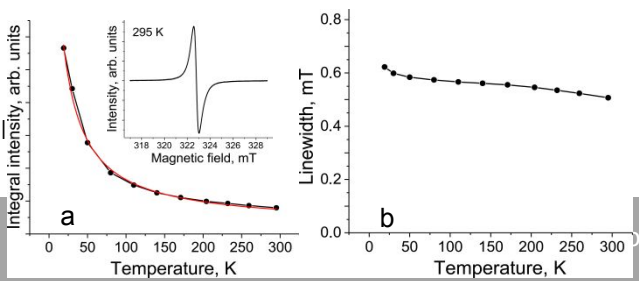

Conflicts of interest

There are no conflicts to declare.

Acknowledgements

The work was supported by FASO Russia, state task 0089-2014-0036 and JSPS KAKENHI Grant Number 26288035 and JST(ACCEL)27(100150500010) project.

Notes and references

1 (a) C. J. Cooksey, *Biotechnic and Histochemistry*, 2007, **82**, 105 – 125; (b) N. Stasiak, W. Kukuła-Koch and K. Głowniak, *Acta Pol Pharm.* 2014, **71**, 215 – 221.

2 (a) M. Irimia-Vlada, E. D. Głowacki, P. A. Troshin, G. Schwabegger, L. Leonat, D. K. Susarova, O. Krystal, M. Ullah, Y. Kanbur, M. A. Bodea, V. F. Razumov, H. Sitter, S. Bauer and N. S. Sariciftci, *Adv. Mater.* 2012, **24**, 375 – 380; b). E. D. Głowacki, G. Voss and N. S. Sariciftci, *Adv. Mater.* 2013, **25**, 6783 – 6800; c). O. Pitayatanakul, T. Higashino, T. Kadoya, M. Tanaka, H. Kojima, M. Ashizawa, T. Kawamoto, H. Matsumoto, K. Ishikawa, T. Mori and *J. Mater. Chem. C*, 2014, **2**, 9311 – 9317.

3 (a) M. Yao, K. Kuratani, T. Kojima, N. Takeichi, H. Senoh and T. Kiyobayashi, *Sci. Rep.* 2014, **4**, 3650; (b) M. Yao, H. Sano, H. Ando and T. Kiyobayashi, *Sci. Rep.* 2015, **5**, 10962.

4 (a) W. Beck, C. Schmidt, R. Wienold, M. Steinmann and B. Wagner, *Angew. Chem. Int. Ed*., 1989, **28**, 1529 – 1531; (b) J. -Y. Wu, C. -H. Chang, P. Thanasekaran, C.- C. Tsai, T.- W. Tseng, G. -H. Lee, S. -M. Peng and K.- L. Lu, *Dalton Trans.* 2008, 6110 – 6112; (c) P. Mondal, M. Chatterjee, A. Paretzki, K. Beyer, W. Kaim and G. K. Lahiri, *Inorg. Chem*., 2016, **55**, 3105 – 3116; (d) D. V. Konarev, S. S. Khasanov, A. V. Kuzmin, A. F. Shestakov, A. Otsuka, H. Yamochi, G. Saito and R. N. Lyubovskaya, *Dalton Trans*. 2016, **45**, 17095 – 17099; (e) F. -S. Guo and R. A. Layfield, *Chem. Commun*. 2017, **53**, 3130 – 3133; (f) D. V. Konarev, L. V. Zorina, S. S. Khasanov, A. F. Shestakov, A. M. Fatalov, A. Otsuka, H. Yamochi, H. Kitagawa and R. N. Lyubovskaya, *Inorg. Chem*. 2018, **57**, 583 – 589; (g) M. Chatterjee, P. Ghosh, K. Beyer, A. Paretzki, J. Fiedler, W. Kaim and G. K. Lahiri, *Chem. Asian J*. 2018, **13**, 118 – 125; (h) D. V. Konarev, A. V. Kuzmin, A. M. Fatalov, S.S. Khasanov, E. I.

This journal is © The Royal Society of Chemistry 20xx

Yudanova and R. N. Lyubovskaya, *Chem. Eur. J.* 2018, **24**, 8415 – 8423.
5 A. Roessler, D. Crettenand, O. Dossenbach, W. Marte and P. Rys, *Electrochimica Acta*, 2002, **47**, 1989 – 1995.
6 (a) P. Süsse, M. Steins and V. Kupcik, *Z. Krystallogr.* 1988, **184**, 269 – 273; (b) F. Kettner, L., J. Schäfer, K. Röder, U. Purgahn, H. Krautscheid, *Acta Crystallogr. Sect E Struct. Rep. Online.* 2011, **67**, o2867.
7 (a) D. V. Konarev, A. V. Kuzmin, S. S. Khasanov, A. Otsuka, H. Yamochi, H. Kitagawa and R. N. Lyubovskaya, *J. Org. Chem.* 2018, **83**, 1861 – 1866; (b) D. V. Konarev, M. A. Faraonov, A. V. Kuzmin, S. S. Khasanov, Y. Nakano, M. S. Batov, S. I. Norko, A. Otsuka, H. Yamochi, G. Saito and R. N. Lyubovskaya, *New J. Chem.* 2017, **41**, 6866 – 6874; (c) D. V. Konarev, S. S. Khasanov, A. A. Goryunkov, S. I. Troyanov, V. A. Brotsman, I. N. Ioffe and R. N. Lyubovskaya, *New J. Chem.* 2019, **43**, 2726-2733; (d) D. V. Konarev, S. S. Khasanov, A. F. Shestakov, A. M. Fatalov, A. Otsuka, H. Yamochi, H. Kitagawa and R. N. Lyubovskaya, *Dalton Trans.* 2017, **46**, 14365 – 14372; (e) D. V. Konarev, M. A. Faraonov, A. V. Kuzmin, A. V. Fatalov, N. G. Osipov, S. S. Khasanov, A. F. Shestakov and R. N. Lyubovskaya, *ChemistrySelect*, 2018, **3**, 4339 – 4343.
8 Crystal data for **1**: $C_{253}H_{308}Cl_{11}K_6N_{26}O_{50}$, F.W. 5137.79, black prism, 0.435×0.234×0.135 mm^3; 120.0(2) K: triclinic, space group $P\bar{1}$, a = 15.2735(5), b = 17.5699(5), c = 25.9540(6) Å, α = 97.646(2), β = 98.970(2), γ = 106.968(3)°, V = 6461.6(3) Å^3, Z = 1, d_{calcd} = 1.320 M gm^{-3}, μ = 0.294 mm^{-1}, F(000) = 2709, $2\theta_{max}$ = 58.888°; 49133 reflections collected, 31764 independent; R_1 = 0.0742 for 15231 observed data [> 2σ(F)] with 3176 restraints and 2132 parameters; wR_2 = 0.1746 (all data); final G.o.F. = 1.005. HKLF5 refinement, twin operation is 180º rotation about [1 -1 1] reciprocal lattice direction, refined twin fraction is 0.1345(3). CCDC 1897094.
9 W. Lüttke, H. Hermann and M. Klessinger, *Angew. Chem. Int. Ed*. 1966, **5**, 598 – 599.
10. R. L. Carlin, 'Magnetochemistry', Springer-Verlag, Heidelberg, 1986.
11. B. Bleaney and K. D. Bowers, *Proc. Roy. Soc. London A*, 1952, **214**, 451 – 465.
12. D. C. Johnston, R. K. Kremer, M. Troyer, X. Wang, A. Klümper, S. L. Bud'ko, A. F. Panchula, P. C. Canfield, *Phys. Rev. B* 2000, **61**, 9558 – 9606.

Graphic for TOC

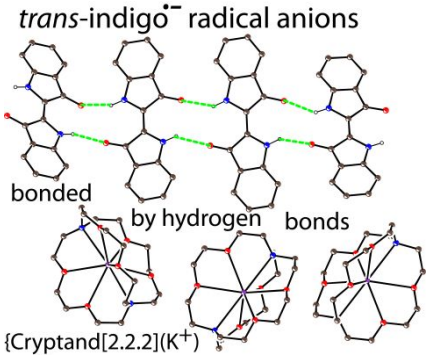

Reduction of *trans*-indigo yields salt {cryptand[2.2.2](K$^+$)}$_6${*trans*-indigo}$_7$· 5.5$C_6H_4Cl_2$ (**1**) with non-integer negative charge on indigo (-0.86). The *trans*-indigo$^{\bullet-}$ radical anions are bonded by intermolecular hydrogen N-H···O=C bonds of 2.11-2.17 Å length which provides rather effective magnetic coupling between *S* = 1/2 spins in **1**.